Final published version available at https://doi.org/10.1016/j.agrformet.2019.107892
© 2020. This manuscript version is made available under the CC-BY-NC-ND 4.0 license
http://creativecommons.org/licenses/by-nc-nd/4.0/

Modeling light below tree canopies overestimates net photosynthesis and radiation use efficiency in understory crops by averaging light in space and time

Adolfo Rosati[a*], Kevin J Wolz[b], Lora Murphy[c], Luigi Ponti[d,e], Shibu Jose[f]

[a] Consiglio per la ricerca in agricoltura e l'analisi dell'economia agraria, centro di ricerca Olivicoltura, Frutticoltura, Agrumicoltura (CREA-OFA), via Nursina 2, 06049 Spoleto (PG), Italy.
[b] Savanna Institute, Madison, Wisconsin 53715 USA
[c] Cary Institute of Ecosystem Studies, Box AB, Millbrook, New York 12545 USA
[d] Agenzia nazionale per le nuove tecnologie, l'energia e lo sviluppo economico sostenibile (ENEA), Centro Ricerche Casaccia, 00123 Rome, Italy
[e] Center for the Analysis of Sustainable Agricultural Systems (CASAS Global www.casasglobal.org), 37 Arlington Avenue, Kensington, CA 94707, USA.
[f] School of Natural Resources, The Center for Agroforestry, University of Missouri, Columbia, MO, USA

* Correspondence: adolfo.rosati@crea.gov.it, CREA, Via Nursina 2, 06049, Spoleto (PG), Italy.
Phone: +39 074349743

Abstract

By averaging in time and/or space, models predict less variable light patterns under tree canopies than in reality. We measured light every minute in 24 positions in a grid under different chestnut orchards, for several clear and overcast days. We also modelled this light with a purposely created 3D, spatially explicit, ray-tracing light interception model, where canopy porosity was calibrated to match measured daily light. Finally, we used both the measured and modeled light patterns transmitted under the tree canopies to estimate the daily net photosynthesis (A_n) and radiation use efficiency (RUE) of an understory wheat leaf. As expected, modeled light was more uniform than measured light, even at equal daily light. This resulted in large overestimation of daily A_n and RUE of the understory leaf. Averaging light in time increased the overestimations even further. A sensitivity analysis showed that this overestimation remained substantial over the range of realistic values for leaf photosynthetic parameters (i.e. $V_{c,max}$, J_{max}, R_d) of the understory crop.

Keywords: agroforestry, alley cropping, leaf response curve, shade tolerance, silvoarable, PAR

Final published version available at https://doi.org/10.1016/j.agrformet.2019.107892
© 2020. This manuscript version is made available under the CC-BY-NC-ND 4.0 license
http://creativecommons.org/licenses/by-nc-nd/4.0/

1. Introduction

Agroforestry systems (AFS) are increasingly recognized for their potential contribution towards sustainable intensification (Doré et al., 2011). Alley cropping (i.e. silvoarable, crops grown in the alleys between lines of trees), is one of the agroforestry practices most studied and developed in temperate regions (Palma et al., 2007; Liagre et al. 2009) because of its potential to increase yield and income while providing environmental benefits and allowing modern mechanization (Dupraz 2005; Garrity et al., 2010; Luedeling et al., 2011; Cardinael et al. 2015). Field experiments in AFS are time-consuming and expensive because of the long-term nature of trees and the many possible combinations of trees and crops (Knörzer et al., 2011; Lovell et al., 2017). Modeling becomes indispensable as an initial test of the many possible field designs and management strategies, improving our understanding of the complex interaction in AFS (Chimonyo et al., 2015). In particular, process-based models are considered particularly suitable (Bayala et al., 2015; Luedeling et al., 2016).

Light is often the most limiting factor in crop growth in AFS (e.g. Friday and Fownes 2002; Jose et al. 2004; Zamora et al. 2009), therefore a proper representation of light distribution between trees and crops becomes essential for effective modeling (Dufour et al., 2013). Light distribution under trees has been addressed with different levels of complexity in different models (for a review, see Malézieux et al., 2009). Initial models considered trees and crops with a single one-dimensional canopy representation, with strong limitations. Two-dimensional models improved upon this, but only three-dimensional (3D), spatially explicit models are suited to represent the highly variable light distribution when combining trees and crops (Chazdon and Pearcy, 1986; Knapp and Smith, 1987).

Only models that reproduce the exact architecture of trees, at the individual shoot or leaf level (e.g. Dauzat et al. 2001; Mialet-Serra et al. 2001; Casella and Sinoquet 2007; Lamanda et al. 2008) can predict the exact light pattern available under the trees in both time and space. While

Final published version available at https://doi.org/10.1016/j.agrformet.2019.107892
© 2020. This manuscript version is made available under the CC-BY-NC-ND 4.0 license
http://creativecommons.org/licenses/by-nc-nd/4.0/

possible, this approach is computationally demanding, making it impossible on a large scale. Therefore, the most common 3D models of AFS approximate light interception by tree canopies using:

1) a fixed geometric shape for the canopy (e.g. cylinder, ellipsoid)
2) a homogeneous canopy of a fixed porosity to light
3) averaging the position of the sun over time

These simplifications result in predictions of light patterns under the trees that are always averaged at some level of time and space, not representing the actual variability.

For a given total light interception, photosynthesis is reduced under variable light compared to more uniform light (Külheim et al., 2002; Poorter et al., 2016; Kromdijk et al., 2016; Vialet-Chabrand et al., 2017). This is because the photosynthetic response of a leaf to light is curvilinear: at high irradiance, net photosynthetic assimilation (A_n) tends to saturate, reducing the radiation use efficiency (RUE). At very low light, the apparent quantum yield is highest, but RUE decreases due to leaf respiration. RUE is zero at the light compensation point and becomes negative at lower irradiance (Hirose and Bazzaz, 1998; Rosati and DeJong, 2003). Therefore, two minutes at average irradiance can result in greater A_n than one minute at high and one at low irradiance.

Work on sunflecks and shadeflecks supports the idea that accounting for the effects of variable light is important not only in understory plants (Pearcy et al., 1996; Way and Pearcy, 2012) but also in common crops (Lawson et al., 2012; Carmo-Silva et al., 2015, Kromdijk et al., 2016), where most of the leaves are still exposed to variable light levels due to self-shading (Pearcy et al., 1990; Rosati et al., 2004). Accounting for the variability in the patterns of incident light is especially important for understory crops in AFS, where the incident light is filtered through tree canopies. Variability in light patterns in AFS is caused by both large gaps between trees and small gaps within tree canopies (Chazdon and Pearcy, 1986; Knapp and Smith, 1987). For an equal total incident radiation transmitted below the trees, different light patterns likely result in different A_n and RUE.

Final published version available at https://doi.org/10.1016/j.agrformet.2019.107892
© 2020. This manuscript version is made available under the CC-BY-NC-ND 4.0 license
http://creativecommons.org/licenses/by-nc-nd/4.0/

Here, we hypothesize that averaging of sub-tree canopy light patterns in time and space overestimates A_n and RUE of understory crops in AFS.

2. Materials and Methods

First, we built a 3D, spatially explicit, ray tracing light interception model with a minutely resolution. While ray-tracing models are commonly used in biophysical modeling, most do not have a minutely resolution. We also measured minutely light transmitted during several days to 24 points in a grid under several chestnut (*Castanea mollissima* Blume) orchards of different ages and spacings. Then, we compared measured and modeled values of light transmitted to the understory crop. Finally, we modeled A_n of a wheat leaf in each of the 24 positions as exposed to (1) the actual (i.e. measured every minute) light pattern transmitted under the trees, (2) temporal averages (half-hourly, hourly, and daily) of the measured light, and (3) modeled (minutely, half-hourly, hourly, and daily) light when approximating the tree crowns to ellipsoids or cylinders. A sensitivity analysis was also performed by changing the photosynthetic parameters of the understory crop to simulate variation in leaf physiology.

2.1 Measuring light under tree canopies in the field

We measured the photosynthetically active radiation (PAR) transmitted under the canopies of four adjacent trees in two mature and two young chestnut orchards differing in age, spacing, and row orientation (Table 1). The orchards were located at the Horticulture and Agroforestry Research Center of the University of Missouri, in New Franklin, MO, USA. The mature orchards were 20 years old, and the young orchards were five years old. Tree characteristics (i.e. trunk circumference, bole height, tree height, within-row canopy radius, and between-row canopy radius) were measured on each of the 16 trees (four per orchard) under which PAR was measured (Table S1). Canopy volumes were then calculated approximating the canopy shape to either an ellipsoid or a cylinder. The trees in the mature orchards were heterogeneous in size, with canopy volumes ranging from 56

Final published version available at https://doi.org/10.1016/j.agrformet.2019.107892
© 2020. This manuscript version is made available under the CC-BY-NC-ND 4.0 license
http://creativecommons.org/licenses/by-nc-nd/4.0/

111 to 135 m^3 in mature orchard A and from 56 to 285 m^3 in mature orchard B. In the young orchards,
112 tree canopy ranged from 8 to 25 m^3 in young orchard A and from 12 to 29 m^3 young orchard B.
113 In each orchard, 24 PAR sensors (GaAsP photosensors, Hamamatsu, Japan), previously
114 calibrated with a quantum sensor (LI-190; LI-COR Inc., Lincoln, NE, USA) and connected to a
115 datalogger (GP2, Delta-T Devices Ltd, Cambridge, UK), were placed in a grid in the rectangular
116 area between the four adjacent trees. The grid was designed with regular spacing to be
117 representative of the whole area. Measurements were made in September and October 2016, over
118 two-five days in each orchard (Table 1), measuring PAR every minute. Daily PAR incident on each
119 orchard was then computed by summing the minutely values for the whole daylight period.
120 Measurement days included clear, partly overcast, and heavily overcast days, as indicated by the
121 total daily incident PAR measured outside the orchard with a PAR sensor (LI-190; LI-COR Inc.,
122 Lincoln, NE, USA) connected to a datalogger recording PAR every minute (Table 1).
123
124 *2.2 Light interception model*
125 Most 3D canopy light interception models do not run on a minutely time scale. Therefore, to
126 compare PAR measured every minute with modeled PAR, we built a model capable of modeling
127 light at any time scale. The model is built using the R statistical computing software version 3.5.1
128 (R Core Team, 2018). The model utilizes a horizontal scene, onto which trees can be placed, and a
129 hemispherical sky discretized into one-degree by one-degree grid cells. The location of the sun and
130 the proportions of direct and diffuse radiation are first calculated using the solaR package
131 (Perpiñán, 2012) using a supplied date, time, and latitude. The proportions of direct and diffuse
132 radiation are calculated following the method of Collares-Pereira and Rabl (1979). Direct radiation
133 is allocated to the sky cell where the sun is located, and diffuse radiation is allocated uniformly
134 across the entire sky. If a day is deemed completely overcast (two days in this study), then both
135 direct and diffuse radiation are allocated uniformly across the entire sky.

Final published version available at https://doi.org/10.1016/j.agrformet.2019.107892
© 2020. This manuscript version is made available under the CC-BY-NC-ND 4.0 license
http://creativecommons.org/licenses/by-nc-nd/4.0/

Tree canopies are placed onto the scene using an x and y location, upper and lower heights of the crown, a uniform canopy porosity (Table 1), and crown radii: two independent radii for an ellipsoid or one uniform radius (i.e. the average of the radii measured in two directions) for a cylinder (Table S1). For a given point of interest on the scene floor, a line is drawn between each sky grid cell and the point. The radiation transmitted to the point is the sum of the radiation of all sky grid cells, with the radiation from a given sky cell reduced by the canopy porosity if its line intersects a tree canopy. Tree canopies are assumed to reduce radiation uniformly regardless of the path length of a radiation ray through the canopy. The effect of tree trunks was assumed negligible during the months of the experiment, as all trees had full foliage (Dupraz et al. 2018). Sensors in the field were placed in a grid within the rectangle between four adjacent trees, avoiding the border of the orchard, to avoid edge effects. Similarly, the model for each orchard included two additional rows of trees in all directions; the dimensions of additional trees in each orchard were taken as the mean of the four primary trees in that orchard.

The purpose of the study was not to assess whether the model could correctly estimate total daily PAR transmitted under the trees, but rather to investigate whether the intra-daily variability of the PAR pattern affects estimation of daily A_n and RUE of an understory crop leaf. Therefore, we set the canopy porosity for each orchard and canopy shape that provided the best match of measured and modeled daily PAR averaged across the 24 sensors (Fig. 1; Table 1). By matching measured and modeled daily PAR, any difference in estimated daily A_n can be attributed to different daily patterns of PAR transmitted under the canopy. The model and the data files are available on GitHub: https://github.com/kevinwolz/Rosati_etal_2019.

2.3 Modeling daily A_n with measured and modeled light

The daily A_n for an understory crop leaf was estimated by using the Farquhar model (Farquhar et al., 1980) with parameters for winter wheat (*Triticum aestivum*; Guo et al., 2015). Wheat was selected because it is the most common crop grown in temperate alley cropping

Final published version available at https://doi.org/10.1016/j.agrformet.2019.107892
© 2020. This manuscript version is made available under the CC-BY-NC-ND 4.0 license
http://creativecommons.org/licenses/by-nc-nd/4.0/

experiments to date (Wolz and DeLucia, 2018). Instantaneous A_n was estimated from instantaneous PAR via eight different approaches: using measured or modeled data, each as measured each minute, or averaged over half-hour, hour, or all daylight hours. Daily A_n for each sensor was then obtained for each calculation approach by summing instantaneous A_n over each day (for further details on this approach see Rosati et al., 2003; 2004). The daily A_n obtained with measured minutely PAR was assumed to be the most realistic, thus all other approaches were compared to this A_n. Daily RUE was then calculated by dividing daily A_n, obtained with the different PAR data, by its respective daily incident PAR.

2.4 Sensitivity analysis

To ensure that results were relevant beyond the specific leaf physiology of winter wheat measured in Guo et al. (2015), a sensitivity analysis of the overestimation of daily A_n in the understory crop to the Farquhar et al. (1980) photosynthesis model parameters was performed. This was done by estimating daily *An* using a range of values for the three key Farquhar et al. (1980) model parameters: (1) $V_{c,max}$, the maximum RuBP saturated rate of carboxylation (μmol m^{-2} s^{-1}), (2) J_{max}, the maximum rate of electron transport used in the regeneration of RuBP (μmol m^{-2} s^{-1}), and (3) R_d, the mitochondrial respiration rate in the day (μmol m^{-2} s^{-1}). The ranges explored for $V_{c,max}$ and R_d were taken from the ranges measured in winter wheat by Sun et al. (2015). Since $V_{c,max}$ and J_{max} are known to be highly correlated across plant species and plant functional types (Wullschleger 1993, Walker et al. 2014), the values explored for J_{max} were calculated from the $V_{c,max}$ values and the relationship demonstrated by Walker et al. (2014).

3. Results

Even though we set the canopy porosity so that total daily modeled and measured PAR below the orchard were matched (Fig. 1), the difference in the daily patterns between measured and modeled minutely data was dramatic.

Final published version available at https://doi.org/10.1016/j.agrformet.2019.107892
© 2020. This manuscript version is made available under the CC-BY-NC-ND 4.0 license
http://creativecommons.org/licenses/by-nc-nd/4.0/

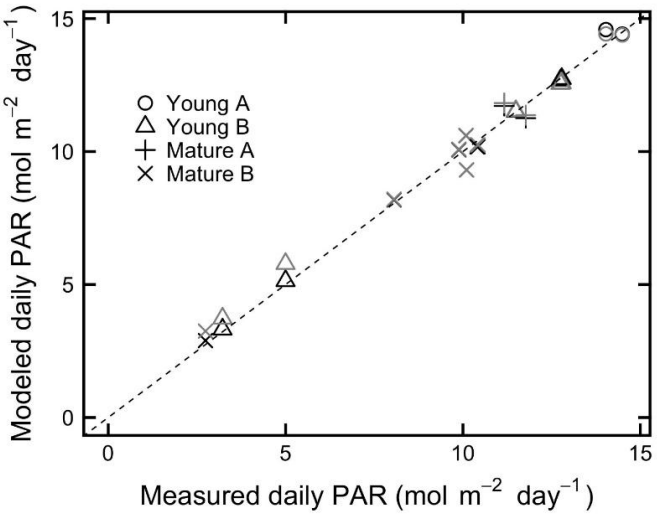

188

189 **Fig. 1** Average modeled vs. measured daily PAR incident on the understory crop across the
190 orchard floor after calibration of the canopy porosity in each orchard. Point shapes represent the
191 different orchards, and point color represent the two modeled canopy geometries (ellipsoid: black;
192 cylinder: grey).

193

194 While generally following the same trends, measured data was much more variable, whereas
195 modeled data maintained smooth curves since the modeled light is passing through unrealistically
196 homogeneous canopies (Fig. 2). Since the results were nearly identical when modeling canopy
197 shape as a cylinder or as an ellipsoid, the rest of results are shown only for one shape (i.e. ellipsoid).

Final published version available at https://doi.org/10.1016/j.agrformet.2019.107892
© 2020. This manuscript version is made available under the CC-BY-NC-ND 4.0 license
http://creativecommons.org/licenses/by-nc-nd/4.0/

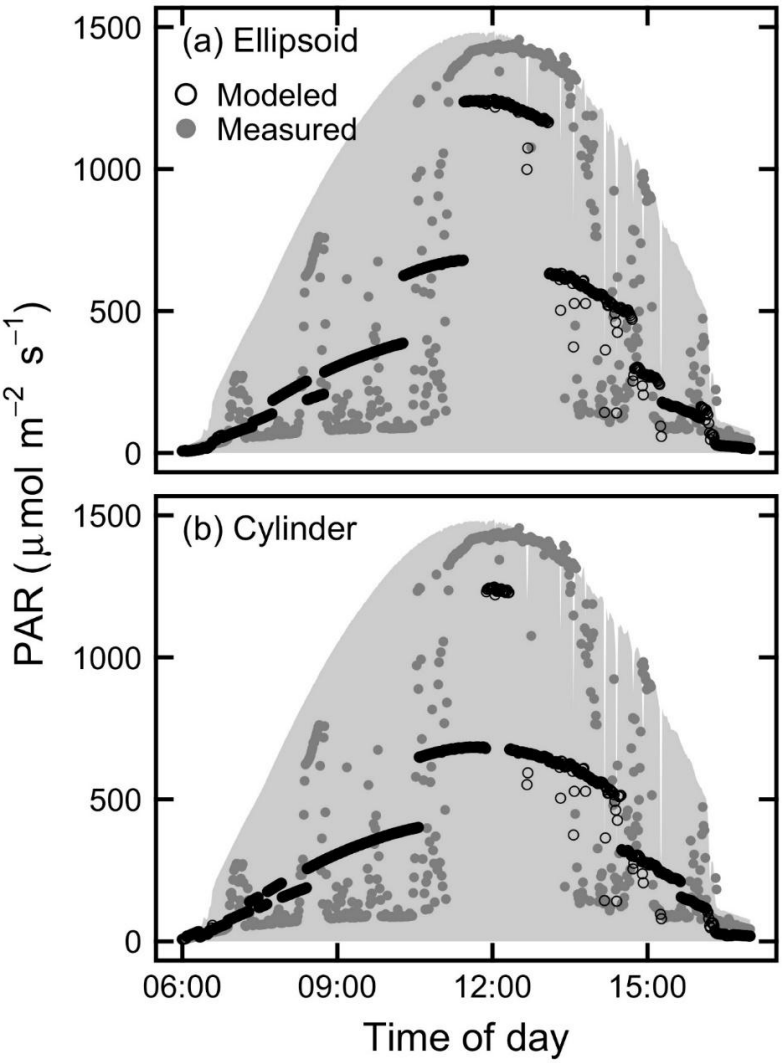

198

199 **Fig. 2** Representative example time series of measured and modeled minutely PAR from one
200 sensor under the canopy in the Young A orchard on a clear day. The shaded area shows the PAR
201 incident on the orchard above the tree canopy. Modeled data is shown for (a) ellipsoidal and (b)
202 cylindrical tree canopies.

203

204

205 A_n always increased with daily incident PAR, both when estimated with measured or with
206 modeled PAR, and when estimated using the minutely PAR data, or the half-hour, hour and daily
207 PAR averages (Fig. 3). However, A_n was always greater at any PAR value when estimated with
208 modeled PAR, both for minutely PAR and at any time averaging level except for daily averages,

Final published version available at https://doi.org/10.1016/j.agrformet.2019.107892
© 2020. This manuscript version is made available under the CC-BY-NC-ND 4.0 license
http://creativecommons.org/licenses/by-nc-nd/4.0/

where it was the same by default design of the modeling (i.e. when using a single PAR value for a day, there is no difference in daily pattern between modeled and measured data, and the response curve takes the shape of the instantaneous response curve). Daily A_n estimated with modeled PAR was also less variable at any given daily PAR. Daily RUE was similarly overestimated with modeled data and more scattered with measured data (Fig. 4).

Final published version available at https://doi.org/10.1016/j.agrformet.2019.107892
© 2020. This manuscript version is made available under the CC-BY-NC-ND 4.0 license
http://creativecommons.org/licenses/by-nc-nd/4.0/

215

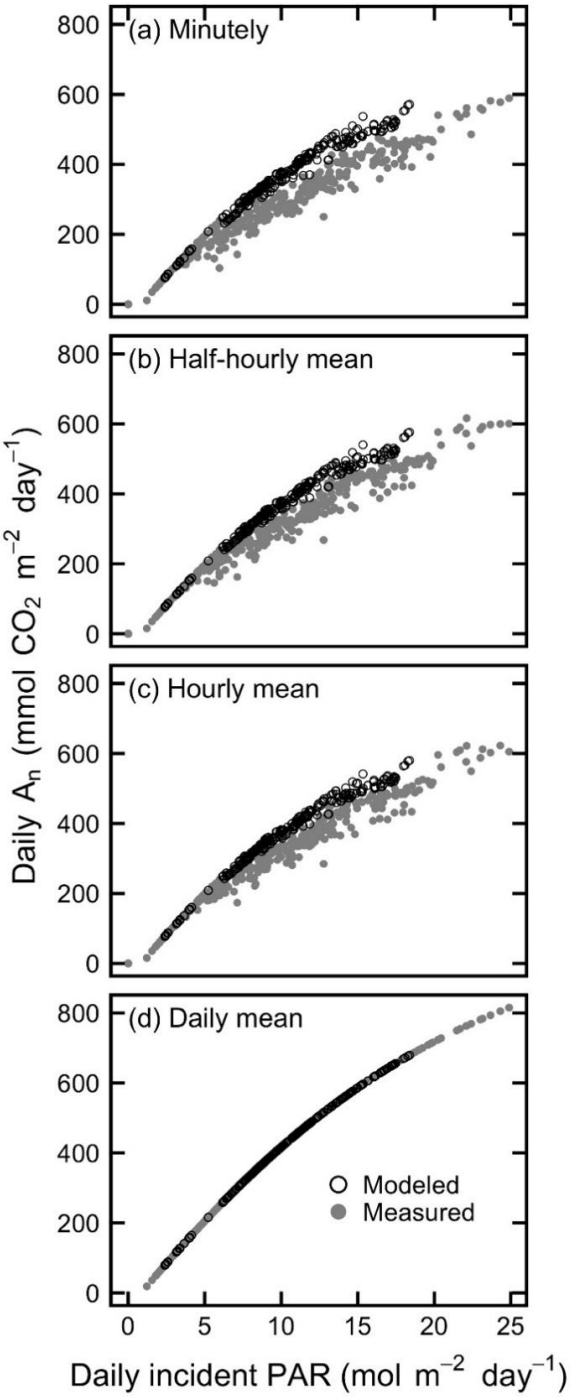

216

217 **Fig. 3** Measured and modeled daily A_n as a function of daily incident PAR. Modeled data is for
218 ellipsoidal tree canopies. Each point represents one of the 24 sensor locations for one of the 11
219 orchard-date combinations measured in the field. Daily A_n is calculated using incident PAR
220 averaged at the (a) minutely, (b) half-hourly, (c) hourly, and (d) daily level.

Final published version available at https://doi.org/10.1016/j.agrformet.2019.107892
© 2020. This manuscript version is made available under the CC-BY-NC-ND 4.0 license
http://creativecommons.org/licenses/by-nc-nd/4.0/

221

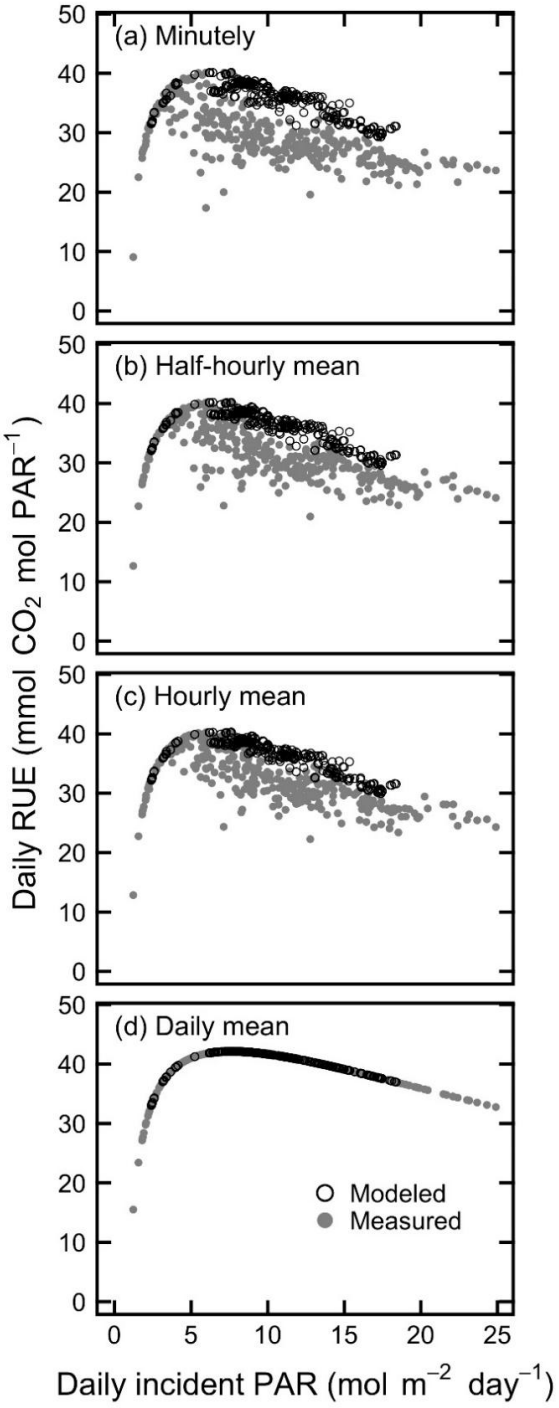

222

223 **Fig. 4** Measured and modeled daily RUE as a function of daily incident PAR. Modeled data is for
224 ellipsoidal tree canopies. Each point represents one of the 24 sensor locations for one of the 11
225 orchard-date combinations measured in the field. Daily RUE is calculated using incident PAR
226 averaged at the (a) minutely, (b) half-hourly, (c) hourly, and (d) daily level.

Final published version available at https://doi.org/10.1016/j.agrformet.2019.107892
© 2020. This manuscript version is made available under the CC-BY-NC-ND 4.0 license
http://creativecommons.org/licenses/by-nc-nd/4.0/

227 Compared to daily A_n estimated using the actual (i.e. measured minutely) PAR, modeled
228 minutely PAR overestimated daily A_n by an average of 26% across all orchards (top right panel;
229 Fig. 5). When temporally averaging the light as well, in addition to the spatial averaging of light
230 inherent in the model (i.e. uniform canopy porosity), the overestimation increased: Half-hourly
231 (28%) and hourly (29%) approaches were only marginally worse, but calculating daily A_n using
232 mean daily modeled PAR resulted in overestimation by 46%. Using temporal averages of measured
233 PAR overestimated daily A_n less than with the corresponding modeled PAR, except for daily
234 averages, with daily A_n overestimations of 7%, 11% and 49% respectively for half-hourly hourly
235 and daily averages (Fig. 5).

Final published version available at https://doi.org/10.1016/j.agrformet.2019.107892
© 2020. This manuscript version is made available under the CC-BY-NC-ND 4.0 license
http://creativecommons.org/licenses/by-nc-nd/4.0/

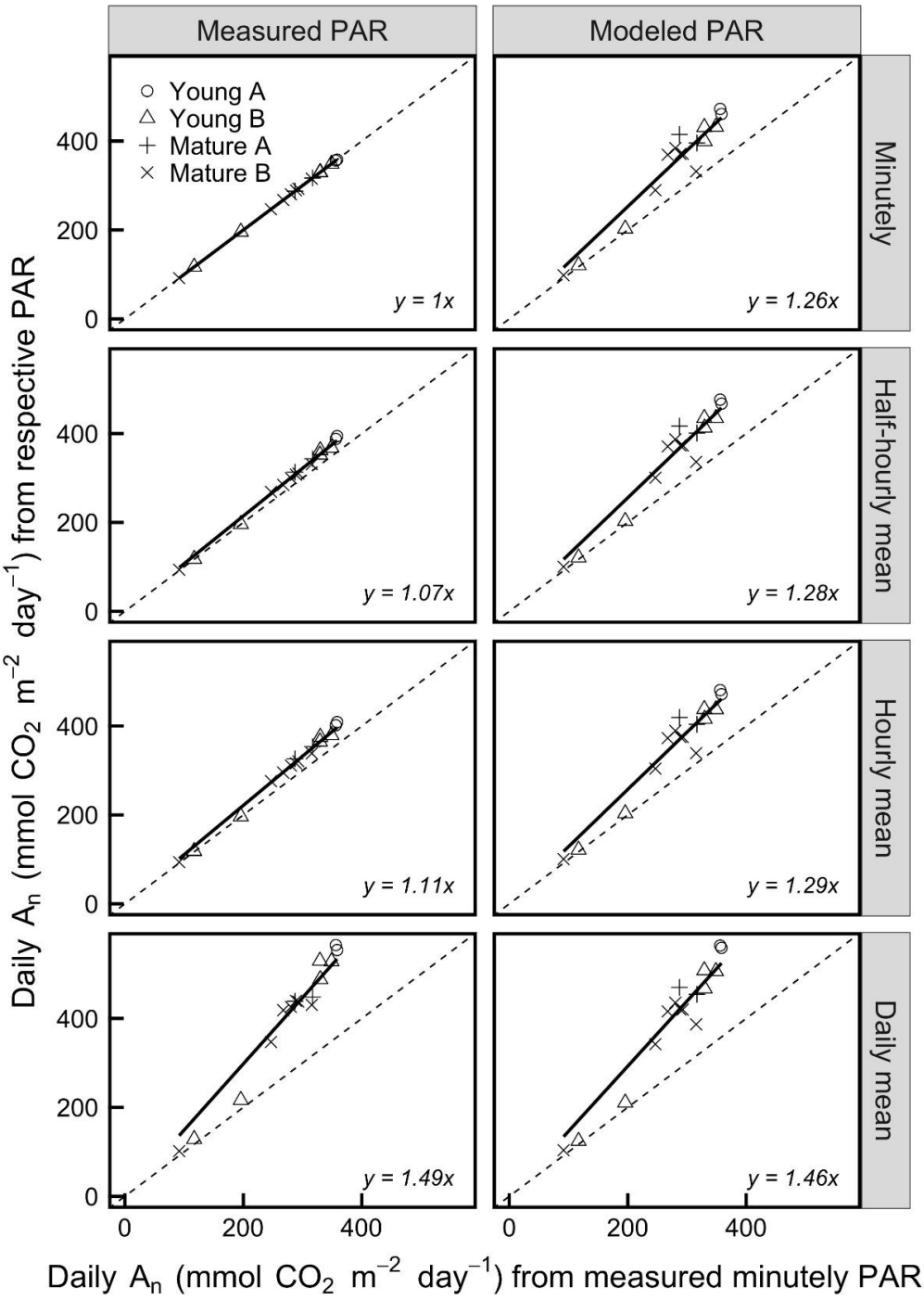

236

237 **Fig. 5** Comparison between daily A_n calculated from measured minutely PAR (x-axis) and daily A_n
238 calculated from measured/modeled PAR in each temporal averaging window. Each point
239 represents the mean of the 24 sensor locations for one of the 11 orchard-date combinations
240 measured in the field.

241 The overestimations of daily A_n resulted in similar overestimations of daily RUE (Fig. 6).

Final published version available at https://doi.org/10.1016/j.agrformet.2019.107892
© 2020. This manuscript version is made available under the CC-BY-NC-ND 4.0 license
http://creativecommons.org/licenses/by-nc-nd/4.0/

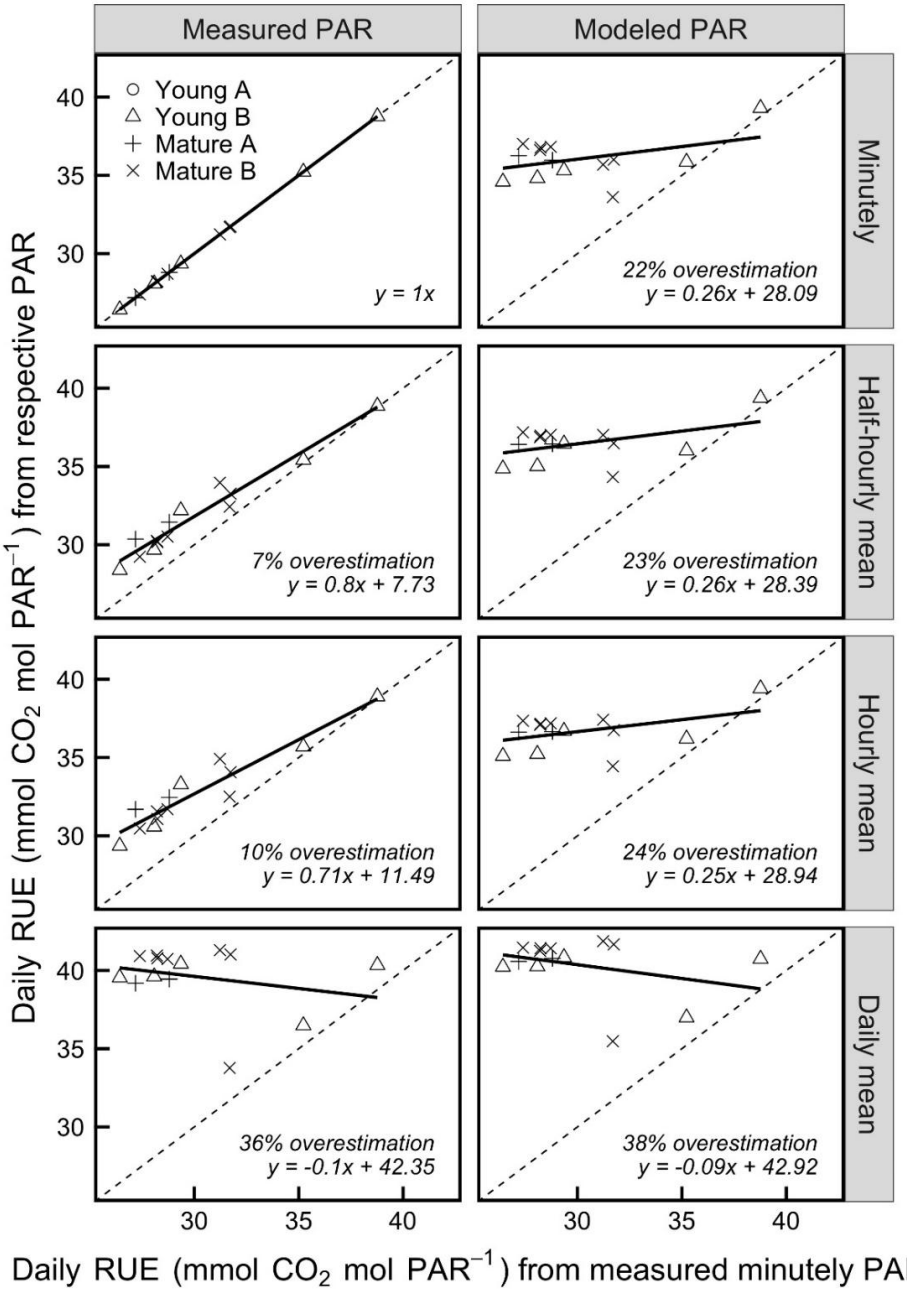

242

243 **Fig. 6** Comparison between daily RUE calculated from measured minutely PAR (x-axis) and daily
244 RUE calculated from measured/modeled PAR in each temporal averaging window. Each point
245 represents the mean of the 24 sensor locations for one of the 11 orchard-date combinations
246 measured in the field.

247 The sensitivity analysis (i.e. estimating A_n with a range of photosynthetic model parameter
248 values for the understory crop) showed that modeling and averaging PAR resulted in large

Final published version available at https://doi.org/10.1016/j.agrformet.2019.107892
© 2020. This manuscript version is made available under the CC-BY-NC-ND 4.0 license
http://creativecommons.org/licenses/by-nc-nd/4.0/

249 overestimation of A_n for any realistic values of the Farquhar et al. (1980) model parameters (i.e.

250 $V_{c,max}$, J_{max} and R_d: Fig. 7).

251

Final published version available at https://doi.org/10.1016/j.agrformet.2019.107892
© 2020. This manuscript version is made available under the CC-BY-NC-ND 4.0 license
http://creativecommons.org/licenses/by-nc-nd/4.0/

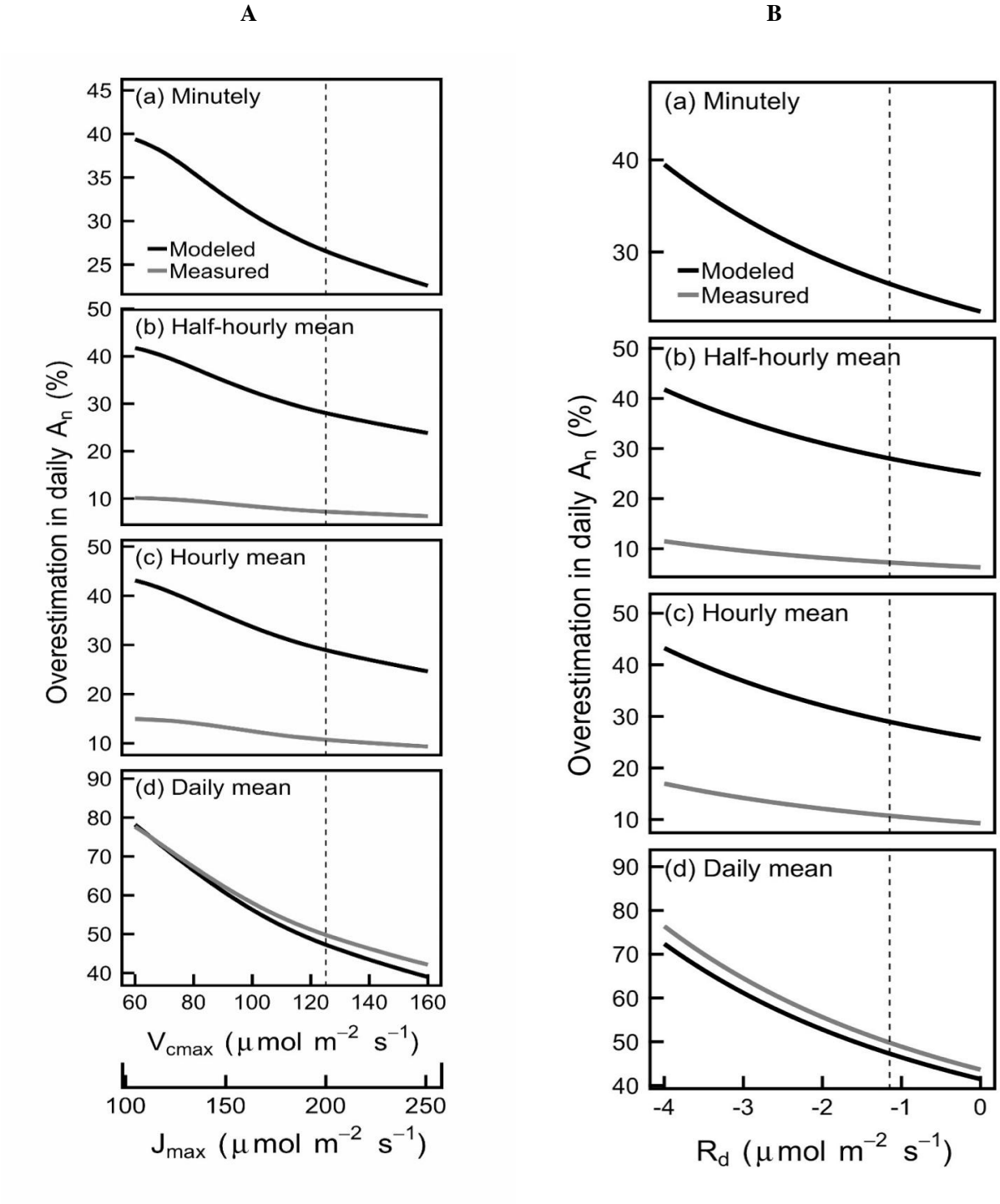

252

253 **Fig. 7** Sensitivity analysis of the overestimation of daily A_n (A) and RUE (B) in the understory crop
254 calculated as in figure 5 and 6, but at varying $V_{c,max}$, J_{max} and R_d parameters of the Farquhar et al.
255 (1980) photosynthesis model. The vertical dotted line represents the parameter values used in all
256 other figures.

Final published version available at https://doi.org/10.1016/j.agrformet.2019.107892
© 2020. This manuscript version is made available under the CC-BY-NC-ND 4.0 license
http://creativecommons.org/licenses/by-nc-nd/4.0/

4. Discussion

Our hypothesis was that, by averaging the PAR transmitted under the tree canopy in space (i.e. by approximating canopy shapes and assuming uniform canopy porosity) and time, crop models overestimate A_n and RUE of understory crops. The results fully supported the hypothesis. Daily A_n estimated with measured minutely PAR was always lower than the A_n estimated using the modeled PAR, even when modeling PAR for every minute (Fig. 3). Averaging in time further increased the overestimation, both for modeled and measured PAR. By comparing daily A_n estimated with measured and modeled PAR at the different time resolutions, the overestimations were shown to be large (Fig. 5). This resulted in similar overestimation of RUE (Fig. 4 and 6). The sensitivity analysis showed that this overestimation remained substantial across realistic values of the Farquhar et al. (1980) photosynthesis model parameters for the understory crop (Fig.7).

It has long been known that averaging of light in space and/or time overestimates A_n (Sinclair et al., 1976; Spitters, 1986). In previous work (Rosati et al., 2003), we also found that averaging measured PAR over one hour resulted in overestimation of daily A_n of different leaves within a tree canopy. However, in a tree or indeed any overstory canopy, most of the photosynthesis is contributed by the outer-canopy, better-exposed leaves, which receive a more uniform irradiance. Understory crops are instead exposed to more variable light patterns even on their outer-canopy leaves. Therefore, quantifying the overestimation of A_n with averaging of light is likely more important. This is the first time that the overestimation is quantified for an understory crop exposed to the PAR transmitted by the overstory canopy, a typical agroforestry situation.

Additionally, our data allowed us to analyze the overestimation due to time and space averaging. Figure 5 shows that daily A_n was overestimated by about 7% when averaging measured PAR data to half-hour intervals, by 11% when averaging hourly, and by 49% when averaging over the entire daylight period. Therefore, time averaging, even at intervals as short as half-hour, results in important overestimations of daily A_n. However, the overestimation was much greater at any time

Final published version available at https://doi.org/10.1016/j.agrformet.2019.107892
© 2020. This manuscript version is made available under the CC-BY-NC-ND 4.0 license
http://creativecommons.org/licenses/by-nc-nd/4.0/

283 averaging step, when using modeled PAR (i.e. approximating tree canopies to regular shape and
284 assuming uniform canopy porosity). When using the modeled PAR at minutely time steps, the
285 overestimation was 26%, more than two or three times the overestimation observed with hourly or
286 half-hourly averages of measured data, respectively.

287 Given that the overestimation results from averaging variable PAR, these results suggest that,
288 at least under the conditions of this experiment, approximating tree canopies to regular shape and
289 assuming uniform canopy porosity results in averaging PAR to a larger extent than hourly time
290 averaging. In fact, it appears clearly that modeled PAR remains at almost constant values for up to
291 three hours, while measured PAR is much more variable (Fig. 2). This suggests that approximating
292 tree canopies to a regular shape and assuming uniform canopy porosity results in greater model bias
293 than setting half-hourly or hourly time steps to save computational effort. This could be due, at least
294 in part, to the fact that our model assumed a regular canopy shape and a uniform canopy porosity,
295 neglecting both clumping (and gaps), and the actual canopy depth crossed by light rays, which
296 depends on where the ray passes (i.e. canopy center or margins). Simple geometrical shapes are
297 very rough approximations of real tree shapes, and leaves are clustered within shoots (Cohen et al.
298 1995; Falster and Welstoby, 2003). Finer geometry descriptions have divided the canopy either in
299 sub-volumes (Mariscal et al. 2000) or voxels (Knyazikhin et al. 1996; Sinoquet et al. 2005). Leaf
300 area distribution within sub-volumes may be considered uniform or described by statistical
301 functions (Wang and Jarvis 1990; Cescatti 1997). Finer canopy descriptions result in dramatic
302 increases in computation time (Mialet-Serra et al. 2001; Roupsard et al. 2008) and, while improving
303 model predictions (Sinoquet et al. 2005), light patterns are still averaged at some levels of space and
304 time. Based on the present results, averaging, even at the scale of relatively short time and/or space
305 intervals, results in important overestimations of daily *An*.

306 For instance, Zhao et al. (2003) accounted for some of these aspects in their model and found
307 the modeled and measured light to be very similar when averaged over half-hour. In this model the
308 actual canopy thickness crossed by each ray was considered, and gaps in the canopy where

Final published version available at https://doi.org/10.1016/j.agrformet.2019.107892
© 2020. This manuscript version is made available under the CC-BY-NC-ND 4.0 license
http://creativecommons.org/licenses/by-nc-nd/4.0/

accounted for by calculating the statistical probability of a ray to pass through the canopy without intercepting a leaf (based on hemispherical photographs). However, this did not yield the actual light available on a given point and time, but rather the "expected average radiation flux on the point". Therefore, while variations in canopy porosity and gap probability were considered, light was still averaged compared to reality. Additionally, canopy shape was still approximated to a regular geometric shape and leaf orientation was assumed to be spherical. Therefore, while better representation of canopy porosity is noteworthy, it probably did not allow measured and modeled transmitted light to match at the instantaneous time scale. Unfortunately, data were presented only as half-hourly averages. At this scale, our results show A_n as overestimated by 7% when using measured PAR, and by 26% when using modeled PAR.

Talbot and Dupraz (2012) also attempted to consider non-uniform canopy porosity, by accounting for clamping with a clumping coefficient, but concluded that this did not improve model predictions of transmitted light. However, this resulted from the fact that the clumping coefficient was too dependent on the canopy volume adjustments procedure. They concluded that their model was not suited to account for the effects of architectural specificities of individual trees. Their results, therefore, do not suggest that more realistic modeling of light transmittance through the canopy is not important, but only that other limitations, particularly the approximation of canopy shape to regular geometric shapes, override possible improvements via other approaches.

Some light models use an explicit stand description at scale of shoot or leaf (Dauzat et al. 2001; Mialet-Serra et al. 2001; Casella and Sinoquet 2007; Lamanda et al. 2008). Models that account for individual leaves are the most likely to predict light patterns under the tree canopy that closely match the actual patterns, but these models are very demanding in terms of the number of parameters needed and computational effort. Consequently, they are not suitable for field agroforestry simulations (many trees), over long time scales.

When using modeled PAR, estimated daily A_n was not only higher but also less variable than when using measured PAR, resulting in a narrower range of A_n values at any daily PAR (Fig.

Final published version available at https://doi.org/10.1016/j.agrformet.2019.107892
© 2020. This manuscript version is made available under the CC-BY-NC-ND 4.0 license
http://creativecommons.org/licenses/by-nc-nd/4.0/

335 3). This trend is also evident for RUE (Fig. 4). In other words, for a given daily incident PAR,
336 measured light results in more variable daily A_n and RUE than for modeled light. This is because a
337 given daily PAR can be obtained with long exposure at uniformly low irradiance or with short
338 alternating exposure at high and low irradiance. In the first case, daily A_n and RUE are higher, while
339 in the second case they are lower, despite having the same daily PAR, because fluctuating
340 irradiance negatively impact time-integrated photosynthesis at equal total irradiance (Külheim et al.,
341 2002; Poorter et al., 2016; Kromdijk et al., 2016; Vialet-Chabrand et al., 2017). By averaging in
342 space and time, modeling PAR reduces the difference in variability in the incident PAR (i.e. more
343 variable light is more affected by averaging than less variable light, which is already closer to an
344 average value), thus not only overestimating daily *An* and RUE but also reducing their variability at
345 any given daily PAR.

346 No current models used in agroforestry account for this variation in A_n and RUE with
347 different sub-canopy light patterns, because all models do some averaging of light in space and/or
348 time. The present results suggest that the light estimation approach used by these models is likely to
349 result in overestimation of A_n and RUE for understory crops. Some models, however, do not use
350 mechanistic approaches (e.g. Farquhar et al. 2018) to estimate A_n in the understory crop, but rather
351 convert daily incident PAR into biomass growth using empirical RUE coefficients. These RUE
352 coefficients are typically measured under field conditions or modeled, calibrated, and validated with
353 field measurements. However, our results show that RUE varies greatly not only with daily PAR,
354 but also with the daily PAR pattern, which, as discussed above, results in quite variable daily *An*
355 and RUE even at equal daily PAR (Fig. 4). The variation of RUE with daily PAR is well
356 established, and the shape of the RUE response curve to daily PAR (Fig. 4) closely resembles the
357 one we previously published (Rosati et al. 2004) or the one often used in modeling (e.g. STICS
358 component in the Hi-SAFe agroforestry model; Brisson et al. 2009, Dupraz et al. 2019). However,
359 in these models, the RUE of the crop is calibrated under full-sun conditions, with a more uniform
360 PAR pattern compared to that experienced under tree canopies. The present work suggests that,

Final published version available at https://doi.org/10.1016/j.agrformet.2019.107892
© 2020. This manuscript version is made available under the CC-BY-NC-ND 4.0 license
http://creativecommons.org/licenses/by-nc-nd/4.0/

361 when such calibrations in open fields are used in the crop component of agroforestry models, they
362 are likely to overestimate the A_n and RUE of the crop under the trees. In this work, with chestnut
363 orchards with different tree ages and spacing, *An* of the understory crop was overestimated by 26-
364 46% (Fig. 5), and RUE by 22-38% (Fig. 6).
365 The impact of these results on global biophysical models is difficult to predict. Most crop-
366 only models are applied only in full-sun situations, and most forest models do not model
367 photosynthesis directly. Nevertheless, considering that agroforestry is practiced on almost half of all
368 agricultural area worldwide (Nair et al. 2009), and there is increasing interest in mixed tree-crop
369 land uses, it will be critical to consider these results to correctly develop global biophysical
370 agroforestry models.
371
372 **5. Conclusions**
373 The current results suggest that modeling understory crop A_n and RUE is quite challenging for
374 several reasons. First, the daily PAR incident over the understory canopy varies from place to place
375 during the same day, therefore the modeling must be done separately for different positions,
376 receiving different daily PAR. Some models account for this by estimating the PAR incident under
377 the trees at various space scales, then using this PAR to run the crop sub-model for each area unit
378 (e.g. STICS crop model in the Hi-sAFe agroforestry model, Dupraz et al., 2019). However, the
379 daily PAR transmitted in each area under the trees estimated by the models is not realistic, being
380 more uniform than in reality, thus probably resulting in overestimated crop RUE.
381 Ideally, therefore, crop RUE should be calculated under real agroforestry situations, using
382 experimental agroforestry setups. While possible, this complicates model calibration, especially
383 considering, as discussed above, that different agroforestry situations result in different light
384 patterns of daily PAR, resulting in substantially different possible RUE values for a given daily
385 PAR (i.e. high variability of RUE for any daily PAR value, Fig. 4). With varying whether
386 conditions (i.e. frequency of sunny and overcast days), seasons (i.e. duration and intensity of

Final published version available at https://doi.org/10.1016/j.agrformet.2019.107892
© 2020. This manuscript version is made available under the CC-BY-NC-ND 4.0 license
http://creativecommons.org/licenses/by-nc-nd/4.0/

radiation), tree age (i.e. canopy size) and relative shade patterns, and position under the trees, the transmitted PAR pattern under the trees can vary greatly even for an equal daily total PAR, resulting in variable RUE values. Therefore, estimating the correct RUE in agroforestry models might be more challenging than previously thought. Possible solutions to overcome these modeling challenges are desirable.

Final published version available at https://doi.org/10.1016/j.agrformet.2019.107892
© 2020. This manuscript version is made available under the CC-BY-NC-ND 4.0 license
http://creativecommons.org/licenses/by-nc-nd/4.0/

Acknowledgements

This work was supported by a Fulbright research scholarship 2016, that was awarded to the first author, allowing him to visit the Center for Agroforestry at the University of Missouri, Columbia, MO, USA, and to collaborate with the other authors. The work was also supported by the European Union's Horizon 2020 Research and Innovation programme under Grant agreement No. 776467 (MED-GOLD project).

References

Bayala, J., Sanou, J., Teklehaimanot, Z., Ouedraogo, S.J., Kalinganire, A., Coe, R., Noordwijk, M. van, 2015. Advances in knowledge of processes in soil–tree–crop interactions in parkland systems in the West African Sahel: A review. Agriculture, Ecosystems & Environment 205, 25–35. https://doi.org/10.1016/j.agee.2015.02.018

Brisson, N., M. Launay, B. Mary, and N. Beaudoin (Eds.) 2009. Conceptual Basis, Formalisations and Parameterization of the STICS Crop Model, 304 pp., Ed. Quae, Versailles, France.

Cardinael, R., Chevallier, T., Barthès, B.G., Saby, N.P.A., Parent, T., Dupraz, C., Bernoux, M., Chenu, C., 2015. Impact of alley cropping agroforestry on stocks, forms and spatial distribution of soil organic carbon — A case study in a Mediterranean context. Geoderma 259–260, 288–299. https://doi.org/10.1016/j.geoderma.2015.06.015

Carmo- Silva, E., Scales, J.C., Madgwick, P.J., Parry, M. a. J., 2015. Optimizing Rubisco and its regulation for greater resource use efficiency. Plant, Cell & Environment 38, 1817–1832. https://doi.org/10.1111/pce.12425

Casella, E., Slnoquet, H., 2007. Botanical determinants of foliage clumping and light interception in two-year-old coppice poplar canopies: assessment from 3-D plant mockups. Annals of Forest Scince 64, 395–404. https://doi.org/10.1051/forest:2007016

Cescatti, A., 1997. Modelling the radiative transfer in discontinuous canopies of asymmetric crowns. I. Model structure and algorithms. Ecological Modelling 101, 263–274.

Final published version available at https://doi.org/10.1016/j.agrformet.2019.107892
© 2020. This manuscript version is made available under the CC-BY-NC-ND 4.0 license
http://creativecommons.org/licenses/by-nc-nd/4.0/

https://doi.org/10.1016/S0304-3800(97)00050-1

Chazdon, R.L., Pearcy, R.W., 1986. Photosynthetic responses to light variation in rainforest species. Oecologia 69, 524–531. https://doi.org/10.1007/BF00410358

Chimonyo, V.G.P., Modi, A.T., Mabhaudhi, T., 2015. Perspective on crop modelling in the management of intercropping systems. Archives of Agronomy and Soil Science 61, 1511–1529. https://doi.org/10.1080/03650340.2015.1017816

Cohen, S., Mosoni, P., Meron, M., 1995. Canopy clumpiness and radiation penetration in a young hedgerow apple orchard. Agricultural and Forest Meteorology 76, 185–200. https://doi.org/10.1016/0168-1923(95)02226-N

Collares-Pereira, M., Rabl, A., 1979. The average distribution of solar radiation-correlations between diffuse and hemispherical and between daily and hourly insolation values. Solar Energy 22, 155–164. https://doi.org/10.1016/0038-092X(79)90100-2

Dauzat, J., Rapidel, B., Berger, A., 2001. Simulation of leaf transpiration and sap flow in virtual plants: model description and application to a coffee plantation in Costa Rica. Agricultural and Forest Meteorology 109, 143–160. https://doi.org/10.1016/S0168-1923(01)00236-2

Doré, T., Makowski, D., Malézieux, E., Munier-Jolain, N., Tchamitchian, M., Tittonell, P., 2011. Facing up to the paradigm of ecological intensification in agronomy: Revisiting methods, concepts and knowledge. European Journal of Agronomy 34, 197–210. https://doi.org/10.1016/j.eja.2011.02.006

Dufour, L., Metay, A., Talbot, G., Dupraz, C., 2013. Assessing Light Competition for Cereal Production in Temperate Agroforestry Systems using Experimentation and Crop Modelling. Journal of Agronomy and Crop Science 199, 217–227. https://doi.org/10.1111/jac.12008

Dupraz, C., 2005. From silvopastoral to silvoarable systems in Europe: sharing concepts, unifying policies. Silvopastoralism and sustainable land management. CAB International, Wallingford 432.

Dupraz, C., Blitz-Frayret, C., Lecomte, I., Molto, Q., Reyes, F., Gosme, M., 2018. Influence of

Final published version available at https://doi.org/10.1016/j.agrformet.2019.107892
© 2020. This manuscript version is made available under the CC-BY-NC-ND 4.0 license
http://creativecommons.org/licenses/by-nc-nd/4.0/

444 latitude on the light availability for intercrops in an agroforestry alley-cropping system.
445 Agroforestry Systems 92:1019–1033. doi: 10.1007/s10457-018-0214-x
446 Dupraz, C., Wolz, K.J., Lecomte, I., Talbot, G., Vincent, G., Mulia, R., Bussière, F., Ozier-
447 Lafontaine, H., Andrianarisoa, S., Jackson, N., Lawson, G., Dones, N., Sinoquet, H.,
448 Lusiana, B., Harja, D., Domenicano, S., Reyes, F., Gosme, M., Van Noordwijk, M., 2019.
449 Hi-sAFe: A 3D Agroforestry Model for Integrating Dynamic Tree–Crop Interactions.
450 Sustainability 11, 2293. https://doi.org/10.3390/su11082293
451 Falster, D.S., Westoby, M., 2003. Leaf size and angle vary widely across species: what
452 consequences for light interception? New Phytologist 158, 509–525.
453 https://doi.org/10.1046/j.1469-8137.2003.00765.x
454 Farquhar, G.D., Caemmerer, S. von, Berry, J.A., 1980. A biochemical model of photosynthetic CO2
455 assimilation in leaves of C3 species. Planta 149, 78–90.
456 https://doi.org/10.1007/BF00386231
457 Friday, J.B., Fownes, J.H., 2002. Competition for light between hedgerows and maize in an alley
458 cropping system in Hawaii, USA. Agroforestry Systems 55, 125–137.
459 https://doi.org/10.1023/A:1020598110484
460 Garrity, D.P., Akinnifesi, F.K., Ajayi, O.C., Weldesemayat, S.G., Mowo, J.G., Kalinganire, A.,
461 Larwanou, M., Bayala, J., 2010. Evergreen Agriculture: a robust approach to sustainable
462 food security in Africa. Food Security 2, 197–214. https://doi.org/10.1007/s12571-010-
463 0070-7
464 Guo, L.P., Kang, H.J., Ouyang, Z., Zhuang, W., Yu, Q., 2015. Photosynthetic parameter estimations
465 by considering interactive effects of light, temperature and CO2 concentration. International
466 Journal of Plant Production 9, 321-345. https://doi.org/10.22069/ijpp.2015.2220
467 Hirose, T., Bazzaz, F.A., 1998. Trade-off Between Light- and Nitrogen-use Efficiency in Canopy
468 Photosynthesis. Annals of Botany 82, 195–202. https://doi.org/10.1006/anbo.1998.0668

Final published version available at https://doi.org/10.1016/j.agrformet.2019.107892
© 2020. This manuscript version is made available under the CC-BY-NC-ND 4.0 license
http://creativecommons.org/licenses/by-nc-nd/4.0/

469 Jose, S., Gillespie, A.R., Pallardy, S.G., 2004. Interspecific interactions in temperate agroforestry.
470 Agroforestry Systems 61:237-255
471 Knapp, A.K., Smith, W.K., 1987. Stomatal and photosynthetic responses during sun/shade
472 transitions in subalpine plants: influence on water use efficiency. Oecologia 74, 62–67.
473 https://doi.org/10.1007/BF00377346
474 Knörzer, H., Grözinger, H., Graeff-Hönninger, S., Hartung, K., Piepho, H.-P., Claupein, W., 2011.
475 Integrating a simple shading algorithm into CERES-wheat and CERES-maize with
476 particular regard to a changing microclimate within a relay-intercropping system. Field
477 Crops Research 121, 274–285. https://doi.org/10.1016/j.fcr.2010.12.016
478 Knyazikhin, Yu., Kranigk, J., Miessen, G., Panfyorov, O., Vygodskaya, N., Gravenhorst, G., 1996.
479 Modelling three-dimensional distribution of photosynthetically active radiation in sloping
480 coniferous stands. Biomass and Bioenergy, Modelling Short Rotation Forestry Growth 11,
481 189–200. https://doi.org/10.1016/0961-9534(96)00010-4
482 Kromdijk, J., Głowacka, K., Leonelli, L., Gabilly, S.T., Iwai, M., Niyogi, K.K., Long, S.P., 2016.
483 Improving photosynthesis and crop productivity by accelerating recovery from
484 photoprotection. Science 354, 857–861. https://doi.org/10.1126/science.aai8878
485 Külheim, C., Ågren, J., Jansson, S., 2002. Rapid Regulation of Light Harvesting and Plant Fitness
486 in the Field. Science 297, 91–93. https://doi.org/10.1126/science.1072359
487 Lamanda, N., Dauzat, J., Jourdan, C., Martin, P., Malézieux, E., 2008. Using 3D architectural
488 models to assess light availability and root bulkiness in coconut agroforestry systems.
489 Agroforestry Systems 72, 63–74. https://doi.org/10.1007/s10457-007-9068-3
490 Lawson, T., Kramer, D.M., Raines, C.A., 2012. Improving yield by exploiting mechanisms
491 underlying natural variation of photosynthesis. Current Opinion in Biotechnology, Food
492 biotechnology - Plant biotechnology 23, 215–220.
493 https://doi.org/10.1016/j.copbio.2011.12.012
494 Liagre, F., Dupraz, C., Angeniol, C., Canet, A., Ambroise, R., 2009. Agroforestry adoption in

Final published version available at https://doi.org/10.1016/j.agrformet.2019.107892
© 2020. This manuscript version is made available under the CC-BY-NC-ND 4.0 license
http://creativecommons.org/licenses/by-nc-nd/4.0/

495 France: a take off. In: World Congress of Agroforestry (ed) Agroforestry—the future of
496 global land use. World Agroforestry Centre, Nairobi, p 118.
497 Lovell, S.T., Dupraz, C., Gold, M., Jose, S., Revord, R., Stanek, E., Wolz, K.J. 2017. Temperate
498 agroforestry research: considering multifunctional woody polycultures and the design of
499 long-term field trials. Agroforestry Systems 263:1–19. doi: 10.1007/s10457-017-0087-4.
500 Luedeling, E., Sileshi, G., Beedy, T., Dietz, J., 2011. Carbon Sequestration Potential of
501 Agroforestry Systems in Africa, in: Kumar, B.M., Nair, P.K.R. (Eds.), Carbon Sequestration
502 Potential of Agroforestry Systems: Opportunities and Challenges, Advances in
503 Agroforestry. Springer Netherlands, Dordrecht, pp. 61–83. https://doi.org/10.1007/978-94-
504 007-1630-8_4
505 Luedeling, E., Smethurst, P.J., Baudron, F., Bayala, J., Huth, N.I., van Noordwijk, M., Ong, C.K.,
506 Mulia, R., Lusiana, B., Muthuri, C., Sinclair, F.L., 2016. Field-scale modeling of tree–crop
507 interactions: Challenges and development needs. Agricultural Systems 142, 51–69.
508 https://doi.org/10.1016/j.agsy.2015.11.005
509 Malézieux, E., Crozat, Y., Dupraz, C., Laurans, M., Makowski, D., Ozier-Lafontaine, H., Rapidel,
510 B., de Tourdonnet, S., Valantin-Morison, M., 2009. Mixing Plant Species in Cropping
511 Systems: Concepts, Tools and Models: A Review, in: Lichtfouse, E., Navarrete, M.,
512 Debaeke, P., Véronique, S., Alberola, C. (Eds.), Sustainable Agriculture. Springer
513 Netherlands, Dordrecht, pp. 329–353. https://doi.org/10.1007/978-90-481-2666-8_22
514 Mariscal, M.J., Orgaz, F., Villalobos, F.J., 2000. Modelling and measurement of radiation
515 interception by olive canopies. Agricultural and Forest Meteorology 100, 183–197.
516 https://doi.org/10.1016/S0168-1923(99)00137-9
517 Mialet-Serra, I., Dauzat, J., Auclair, D., 2001. Using plant architectural models for estimation of
518 radiation transfer in a coconut-based agroforestry system. Agroforestry Systems 53, 141–
519 149. https://doi.org/10.1023/A:1013320419289
520 Nair, P.K.R., Kumar, B.M., Nair, V.D. 2009. Agroforestry as a strategy for carbon sequestration.

Final published version available at https://doi.org/10.1016/j.agrformet.2019.107892
© 2020. This manuscript version is made available under the CC-BY-NC-ND 4.0 license
http://creativecommons.org/licenses/by-nc-nd/4.0/

521 Journal of Plant Nutrition and Soil Science 172, 10–23
522 Palma, J., Graves, A.R., Burgess, P.J., van der Werf, W., Herzog, F., 2007. Integrating
523 environmental and economic performance to assess modern silvoarable agroforestry in
524 Europe. Ecological Economics, Sustainability and Cost-Benefit Analysis 63, 759–767.
525 https://doi.org/10.1016/j.ecolecon.2007.01.011
526 Pearcy, R.W., Krall, J.P., Sassenrath-Cole, G.F., 1996. Photosynthesis in Fluctuating Light
527 Environments, in: Baker, N.R. (Ed.), Photosynthesis and the Environment, Advances in
528 Photosynthesis and Respiration. Springer Netherlands, Dordrecht, pp. 321–346.
529 https://doi.org/10.1007/0-306-48135-9_13
530 Pearcy, R.W., Roden, J.S., Gamon, J.A., 1990. Sunfleck dynamics in relation to canopy structure in
531 a soybean (Glycine max (L.) Merr.) canopy. Agricultural and Forest Meteorology 52, 359–
532 372. https://doi.org/10.1016/0168-1923(90)90092-K
533 Perpiñan Lamigueiro, O., 2012. solaR: Solar Radiation and Photovoltaic Systems with R. Journal of
534 Statistical Software 50, 1–32.
535 Poorter, H., Fiorani, F., Pieruschka, R., Wojciechowski, T., Putten, W.H. van der, Kleyer, M.,
536 Schurr, U., Postma, J., 2016. Pampered inside, pestered outside? Differences and similarities
537 between plants growing in controlled conditions and in the field. New Phytologist 212, 838–
538 855. https://doi.org/10.1111/nph.14243
539 Rosati, A., Dejong, T.M., 2003. Estimating Photosynthetic Radiation Use Efficiency Using Incident
540 Light and Photosynthesis of Individual Leaves. Annals of Botany 91, 869–877.
541 https://doi.org/10.1093/aob/mcg094
542 Rosati, A., Metcalf, S.G., Lampinen, B.D., 2004. A Simple Method to Estimate Photosynthetic
543 Radiation Use Efficiency of Canopies. Annals of Botany 93, 567–574.
544 https://doi.org/10.1093/aob/mch081
545 Roupsard, O., Dauzat, J., Nouvellon, Y., Deveau, A., Feintrenie, L., Saint-André, L., Mialet-Serra,
546 I., Braconnier, S., Bonnefond, J.-M., Berbigier, P., Epron, D., Jourdan, C., Navarro, M.,

Final published version available at https://doi.org/10.1016/j.agrformet.2019.107892
© 2020. This manuscript version is made available under the CC-BY-NC-ND 4.0 license
http://creativecommons.org/licenses/by-nc-nd/4.0/

547 Bouillet, J.-P., 2008. Cross-validating Sun-shade and 3D models of light absorption by a
548 tree-crop canopy. Agricultural and Forest Meteorology 148, 549–564.
549 https://doi.org/10.1016/j.agrformet.2007.11.002
550 Sinclair, T.R., Murphy, C.E., Knoerr, K.R., 1976. Development and Evaluation of Simplified
551 Models for Simulating Canopy Photosynthesis and Transpiration. Journal of Applied
552 Ecology 13, 813–829. https://doi.org/10.2307/2402257
553 Sinoquet, H., Sonohat, G., Phattaralerphong, J., Godin, C., 2005. Foliage randomness and light
554 interception in 3-D digitized trees: an analysis from multiscale discretization of the canopy.
555 Plant, Cell & Environment 28, 1158–1170. https://doi.org/10.1111/j.1365-
556 3040.2005.01353.x
557 Spitters, C.J.T., Toussaint, H.A.J.M., Goudriaan, J., 1986. Separating the diffuse and direct
558 component of global radiation and its implications for modeling canopy photosynthesis Part
559 I. Components of incoming radiation. Agricultural and Forest Meteorology 38, 217–229.
560 https://doi.org/10.1016/0168-1923(86)90060-2
561 Sun, Jingsong, Sun, Jindong, Feng, Z., 2015. Modelling photosynthesis in flag leaves of winter
562 wheat (Triticum aestivum) considering the variation in photosynthesis parameters during
563 development. Functional Plant Biology 42, 1036–1044. https://doi.org/10.1071/FP15140
564 Talbot, G., Dupraz, C., 2012. Simple models for light competition within agroforestry
565 discontinuous tree stands: are leaf clumpiness and light interception by woody parts relevant
566 factors? Agroforestry Systems 84, 101–116. https://doi.org/10.1007/s10457-011-9418-z
567 Team, R.C., 2017. R: A language and environment for statistical com-puting. R Foundation for
568 Statistical Computing, Vienna, Austria.
569 Vialet-Chabrand, S., Matthews, J.S.A., Simkin, A.J., Raines, C.A., Lawson, T., 2017. Importance of
570 Fluctuations in Light on Plant Photosynthetic Acclimation. Plant Physiology 173, 2163–
571 2179. https://doi.org/10.1104/pp.16.01767

Final published version available at https://doi.org/10.1016/j.agrformet.2019.107892
© 2020. This manuscript version is made available under the CC-BY-NC-ND 4.0 license
http://creativecommons.org/licenses/by-nc-nd/4.0/

572 Walker, A.P., Beckerman, A.P., Gu, L., Kattge, J., Cernusak, L.A., Domingues, T.F., Scales, J.C.,
573 Wohlfahrt, G., Wullschleger, S.D., Woodward, F.I. 2014. The relationship of leaf
574 photosynthetic traits–Vcmax and Jmax–to leaf nitrogen, leaf phosphorus, and specific leaf
575 area: a meta- analysis and modeling study. Ecology and evolution, 4(16), pp.3218-3235
576 Wang, Y.P., Jarvis, P.G., 1990. Description and validation of an array model — MAESTRO.
577 Agricultural and Forest Meteorology 51, 257–280. https://doi.org/10.1016/0168-
578 1923(90)90112-J
579 Way, D.A., Pearcy, R.W., 2012. Sunflecks in trees and forests: from photosynthetic physiology to
580 global change biology. Tree Physiology 32, 1066–1081.
581 https://doi.org/10.1093/treephys/tps064
582 Wolz, K.J., DeLucia, E.H., 2018. Alley cropping: Global patterns of species composition and
583 function. Agriculture, Ecosystems & Environment 252, 61–68.
584 https://doi.org/10.1016/j.agee.2017.10.005
585 Wullschleger, S.D. 1993. Biochemical limitations to carbon assimilation in C3 plants—a
586 retrospective analysis of the A/Ci curves from 109 species. Journal of experimental botany,
587 44(5), pp.907-920
588 Zamora, D.S., Jose, S., Jones, J.W., Cropper, W.P., 2009. Modeling cotton production response to
589 shading in a pecan alleycropping system using CROPGRO. Agroforestry Systems 76, 423–
590 435. https://doi.org/10.1007/s10457-008-9166-x
591 Zhao, W., Qualls, R.J., Berliner, P.R., 2003. Modeling of the short wave radiation distribution in an
592 agroforestry system. Agricultural and Forest Meteorology 118, 185–206.
593 https://doi.org/10.1016/S0168-1923(03)00108-4
594

Final published version available at https://doi.org/10.1016/j.agrformet.2019.107892
© 2020. This manuscript version is made available under the CC-BY-NC-ND 4.0 license
http://creativecommons.org/licenses/by-nc-nd/4.0/

595

596 **Table 1.** Tree spacing, row orientation, daily incident PAR in the different measuring days, and
597 calibrated tree porosity for the four chestnut orchards used to measure the transmitted PAR on 24
598 positions under the canopies, during several days per orchard.

	Tree spacing (m)		Row orientation (˚E of N)	Daily incident PAR above orchard canopy (mol m^{-2})	Calibr.tree canopy porosity	
Orchard	Within rows	Between rows			Ellipsoid	Cylinder
Mature A	9.3	8.2	168	36.5, 38.6	0.48	0.38
Mature B	8	8	131	31.6, 23.7, 27.3, 30.8, 30.9, 8.3	0.60	0.51
Young A	4	6.5	0	36.4, 37.2	0.47	0.47
Young B	4	6.5	0	9.3, 14.4, 31.6, 34.0, 34.4	0.54	0.49

599

Final published version available at https://doi.org/10.1016/j.agrformet.2019.107892
© 2020. This manuscript version is made available under the CC-BY-NC-ND 4.0 license
http://creativecommons.org/licenses/by-nc-nd/4.0/

600 **Table S1** Tree parameters for the 16 trees used in each of the four orchards.

Orchard	Trunk Circumfer. (cm)	Bole Height (m)		Canopy Height (m)		Canopy Diameter (m)		Canopy Volume (m^3)	
		Cylin	Ellips	Cylin	Ellips	Y	X	Cylin	Ellip
Mature A	62	2.2	1.7	7.0	8.0	4.6	5.0	86.8	75.8
	72	1.8	1.3	5.0	6.0	6.3	6.2	98.1	96.1
	67	1.8	1.3	7.0	8.0	5.5	6.0	135.0	115.7
	63	2.5	2.0	5.0	6.0	5.1	5.6	56.2	59.8
Mature B	63	2.5	2.0	5.0	6.0	5.1	5.6	56.2	59.8
	113	2.5	2.0	8.5	9.5	8.3	6.8	268.5	221.5
	78	1.9	1.4	7.5	8.5	6.0	6.8	180.1	151.6
	111	2.3	1.8	7.5	8.5	8.5	8.2	284.6	244.4
Young A	30	1.5	1.0	3.5	4.5	2.5	2.1	8.3	9.6
	34	1.0	0.5	3.5	4.5	2.5	3.0	14.8	15.7
	30	1.0	0.5	3.5	4.5	2.5	2.5	12.3	13.1
	31	0.8	0.3	3.5	4.5	3.3	3.6	25.2	26.1
Young B	30	1.0	0.5	3.5	4.5	2.5	2.5	12.3	13.1
	31	0.8	0.3	3.5	4.5	3.3	3.6	25.2	26.1
	38	1.0	0.5	3.5	4.5	4.0	3.7	29.1	31.0
	29	1.0	0.5	3.5	4.5	2.5	2.4	11.8	12.6

601